Journal of GeoEngineering, Vol. 17, No. 4, pp. 207-220, December 2022
http://dx.doi.org/10.6310/jog.202212_17(4).4

EXPERIMENTAL STUDY OF ACTIVE EARTH PRESSURES ON RETAINING WALLS ADJACENT TO INCLINED ROCK FACES

Yung-Show Fang [1*], Chia-Cheng Fan [2], Sheng-Feng Huang [3], and Cheng Liu [4]

ABSTRACT

This paper presents the experimental data of lateral earth pressure acting on a vertical rigid wall, which moved away from a constrained backfill of dry sand. An instrumented retaining-wall facility was used to investigate the effects of an adjacent inclined rock face on the development of active earth pressure. Note only loose Ottawa sand was used as backfill material and only the translational mode of wall movement was investigated. Based on the experimental data, it has been found that for the wall with a nearby inclined rock face, the active earth pressure measured at the upper part of the wall was in good agreement with Coulomb's prediction. However, the active pressure measured at the lower part of the wall was lower than Coulomb's prediction. The magnitude of the active soil force decreased with increasing rock face inclination angle, and the point of application of the active resultant ascended with increasing rock face inclination angle. If the inclined rock face was vertical and located very close to the retaining wall, only a narrow backfill was sandwiched between the rock face and the retaining wall. It was impossible for the active soil wedge to develop behind the wall. Consequently, the active pressure distribution was much less than Coulomb's prediction. Calculations based on Coulomb's theory could significantly overestimate the active soil force and the overturning moment.

Key words: Active earth pressure, constrained backfill, model test, retaining wall, sand.

1. INTRODUCTION

The calculation of forces exerted by soils against structures was one of the oldest problems in soil mechanics. The most widely accepted theories to estimate active earth pressure are those of Coulomb and Rankine. For the gravity wall shown in Fig. 1, the Rankine active soil wedge is bounded by the wall and the failure plane with the inclination angle of 45° + ϕ/2 with the horizon, where ϕ is the friction angle of the soil.

If the retaining wall is constructed adjacent to an inclined rock face as shown in Fig. 1, the stiff rock face would intrude the active soil wedge as the wall moves away from the backfill. Can the Coulomb and Rankine theories be used to estimate the active earth pressure on the wall with constrained backfill? Would the distribution of active earth pressure still be linear with depth? To correctly calculate the factor of safety against sliding and overturning of the wall, it is necessary for the designer to understand how would the nearby rock face influence the active earth pressure. In Fig. 1, the inclination angle of the rock face with the horizontal is defined as β, and the horizontal spacing between the bottom of the inclined rock face and the vertical wall face is expressed as *b*. Theoretically, for $b = 0$, if the β angle is less than 45° + ϕ/2, the wedge theory of Coulomb still can be used. However, if the β angle is greater than 45° + ϕ/2, the inclined rock face would intrude the active soil wedge and it might affect the active earth pressure on the wall.

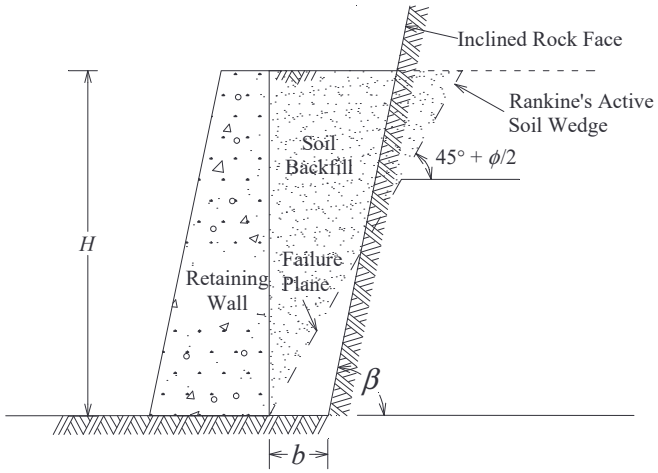

Fig. 1 Intrusion of a rock face into active soil wedge

Valuable studies associated with earth pressure on retaining walls with constrained backfill had been conducted. Based on the arching theory, Spangler and Handy (1984) developed the following theoretical equation for calculating the lateral earth pressure σ_h acting on the wall of a silo:

$$\sigma_h = \frac{\gamma B}{2\mu}\left[1 - e^{-2K\mu(z/B)}\right] \tag{1}$$

where $\mu = \tan\delta$, and δ is the friction angle between the soil and the wall; γ = unit weight of the soil; *B* = backfill width; *K* = coefficient of lateral earth pressure; and *z* = backfill depth. The granular particles in the silo were constrained by the vertical silo

Manuscript received July 27, 2022; revised August 30, 2022; accepted October 5, 2022.
[1*] Professor Emeritus (corresponding author), Department of Civil Engineering, National Yang Ming Chiao Tung University, Hsinchu City 30093, Taiwan (e-mail: ysfang@nycu.edu.tw).
[2] Professor, Department of Construction Engineering, National Kaohsiung University of Science and Technology, Kaohsiung City 82445, Taiwan.
[3] Geotechnical Engineer, Mass Transit Engineering Department, Sinotech Engineering Consultants, Taipei 10570, Taiwan.
[4] Senior Engineer, Department of Rapid Transit Engineering, CECI Engineering Consultants, Inc., Taipei 11491, Taiwan.

walls. Based on the limit equilibrium method and the computer program ReSSA 2.0, Leshchinsky *et al.* (2004) numerically investigated the lateral earth pressure on a mechanically stabilized earth (MSE) retaining wall with constrained fill. Yang and Liu (2007) conducted finite element analysis to study the earth pressures for retaining walls of narrow backfill width for both at-rest and active conditions. Fan and Fang (2010) used the non-linear finite element program PLAXIS to investigate the earth pressure for a rigid wall near an inclined rock face. It was found that the active earth pressure for a wall built with limited backfill space is considerably less than that of the Coulomb solution. The coefficient of active earth pressure is as low as 0.5-0.6 times the Coulomb solution. Using the finite element method, Chen *et al.* (2019a) investigated the active earth pressure acting on the retaining wall with a narrow backfill under the translational mode. Numerical results indicated that, due to the boundary conditions, reflective shear bands occurred in the backfill when the soil reached failing. Based on their finite element analysis, Chen *et al.* (2019b) concluded that, when the retaining wall movement was translational, one to three slip surfaces would develop from the wall heel, and eventually developed to the surface along the soil-wall or soil-rock interface. The coefficient of active earth pressure was as low as 0.5-0.7 times the Coulomb solution and locations (h/H) of the active soil thrust ranged from 0.34 to 0.44. Based on differential slice method and soil arching, Xie *et al.* (2020) proposed analytical solutions for the active soil pressure on retaining walls, which were built near rock faces. It should be noted that, all analytical and numerical investigation mentioned above lacks solid experimental justification.

Frydman and Keissar (1987) used the centrifuge modeling technique to test a small model wall near a vertical rock face. The centrifuge system can develop a maximum acceleration of 100 g, where g is acceleration due to gravity. The aluminum model retaining wall is 195 mm-high, 100 mm-wide and 20 mm-thick. It was reported that the measured K_a value was significantly less than the Rankine's or Coulomb's coefficient of active earth pressure. Take and Valsangkar (2001) conducted centrifuge model tests to investigate the reduction of earth pressure behind retaining walls of narrow backfill width. Earth pressure cells were mounted with epoxy on the 150 mm-high, 254 mm-wide and 12.5 mm-thick aluminum model wall. It was concluded that, with the reduction in backfill width B, arching was observed to truncate lateral earth pressure within the narrow backfill. As predicted by arching theory, the z/B ratio has a dominant effect on the magnitude of the reduction of earth pressure. Unfortunately, little justification based on 1-g physical model tests has been reported in the literature regarding the development of active earth pressure against a wall near an inclined rock face.

This paper presents experimental data associated with the lateral earth pressure against a vertical rigid wall, which moved away from a constrained backfill of dry sand. Note only loose Ottawa sand was used as backfill material and only the translational mode of wall movement was investigated. All of the earth-pressure experiments mentioned in this paper were conducted in the National Yang Ming Chiao Tung University retaining-wall facility which is described in the following section. Horizontal earth pressure against the wall was measured with the soil-pressure transducers mounted on the model wall. A steel interface plate was designed and constructed to simulate the inclined rock face near the retaining wall. Experimental results obtained with the 1-g physical model tests were compared with theoretical solutions, numerical findings and centrifuge test results. It is hoped that these results will enhance a better understanding regarding the influence of a nearby inclined rock face on the development of active earth pressure.

The earth pressure acting on the wall could be influenced by many parameters, for example: the type of wall movement (at-rest, active or passive), mode of wall movement (sliding, overturning, *etc.*), type of wall material (concrete, steel, *etc.*), type of backfill material, density of backfill (loose, medium dense, or dense), inclination angle of backfill surface, and roughness and location of adjacent rock face. To limit the scope of this study, except the parameters b and β regarding the location of the adjacent rock face, all other parameters were kept unchanged. So that the effects of the adjacent rock face on active earth pressure can be clearly identified.

2. RETAINING-WALL FACILITY

The entire facility consists of four components: model retaining wall, soil bin, driving system, and data acquisition system. The movable model retaining wall and its driving system are illustrated in Fig. 2. The model wall is a 1,000-mm-wide, 550-mm-high, and 120-mm-thick solid plate, and is made of steel. Note that in Fig. 2, the effective wall-height H (or height of backfill above wall base) is only 500 mm. The retaining wall is vertically supported by two unidirectional rollers, and is laterally supported by four driving rods. The 1,000 mm-wide, 337 mm-high, and 120 mm-thick steel plate on top of the movable wall is designed to resist the uplift component of passive earth pressure. However, only active earth pressure experiments were conducted for this study. To investigate the distribution of earth pressure, soil pressure transducers (SPTs) were attached to the model retaining wall as shown in Fig. 3. Nine strain-gage-type earth pressure transducers have been arranged within the central zone of the wall. The Kyowa model BE-2KRS17 (196 kN/m^2 capacity) transducer was used for these experiments. In Fig. 3, soil pressure transducers SPT1 to SPT9 used to measure lateral soil pressure on the wall were indicated with black circles. Since SPT0 was installed at the surface level of the backfill (depth $z = 0$), therefore the overburden vertical stress and horizontal stress at this point are always equal to zero. The empty circle in Fig. 3 indicates that the SPT0 is a dummy transducer, which does not measure any soil pressure.

The soil bin is fabricated of steel members with inside dimensions of 2,000 mm × 1,000 mm × 1,000 mm. Both sidewalls of the soil bin are made of 30-mm-thick transparent acrylic plates. As illustrated in Fig. 2, the variable speed motors M1 and M2 (Electro, M4621AB) are employed to propel the upper and lower driving rods, respectively. The shaft rotation propels the worm gear linear actuators, while the actuator would pull the model wall. Since only the variation of earth pressure caused by the translational wall movement (T mode) was investigated, the motor speeds at M1 and M2 were kept the same for all experiments in this study.

Due to the considerable amount of data collected by the soil-pressure transducers, a data acquisition system was used. An analog-to-digital converter digitized the analog signals from the sensors. The digital data were then stored and processed by a microcomputer. For more details regarding the retaining-wall facility, the reader is referred to Fang *et al.* (1994, 2002).

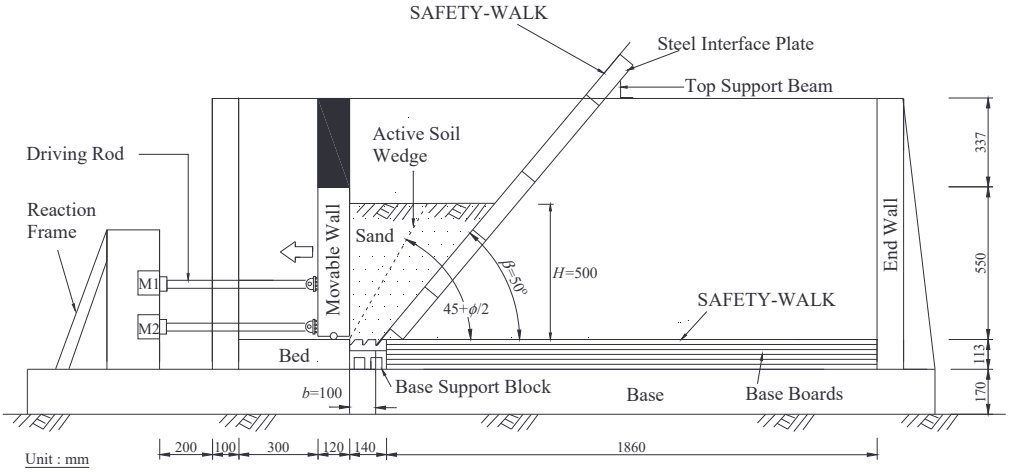

Fig. 2 Model wall test with b = 100 mm and β = 50°

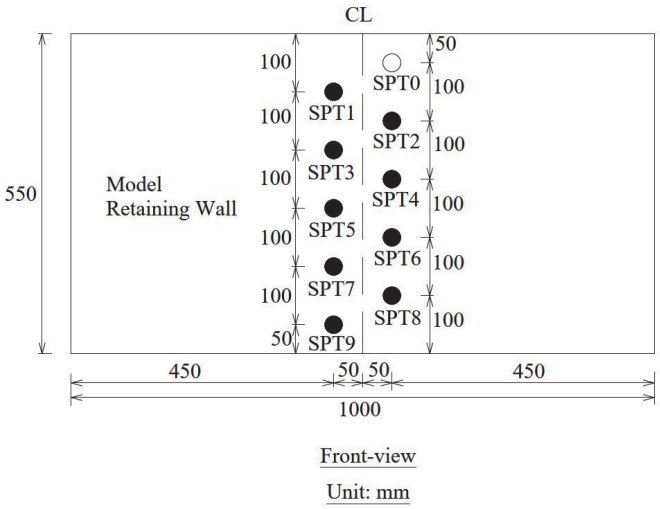

Fig. 3 Locations of soil pressure transducers

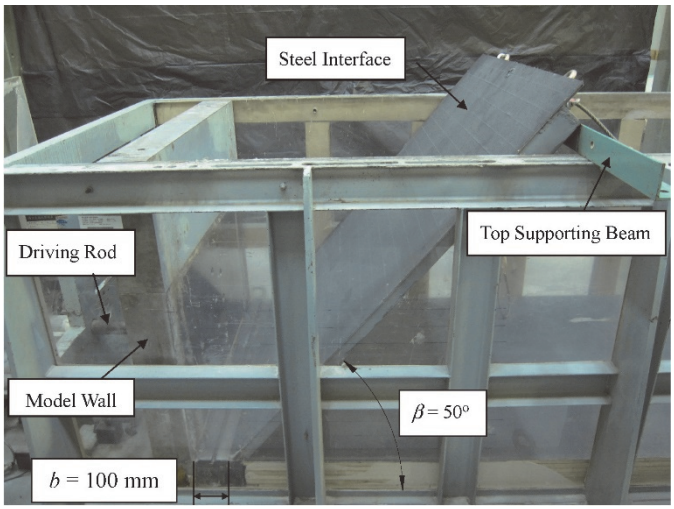

Fig. 4 Model wall test with interface inclination β = 50° and b = 100 mm

2.1 Interface Plate

A steel interface plate was designed and constructed to simulate the inclined rock face near the retaining wall shown in Fig. 1. The plate and its supporting system were developed to fit in the model retaining-wall facility. A picture of the model retaining wall and the steel interface plate was shown in Fig. 4.

The steel interface plate shown in Fig. 2 is 1,370 mm-long, 998 mm-wide, and 5 mm-thick. In Fig. 4, a layer of anti-slip material (SAFETY-WALK, 3M) was attached to the plate surface to simulate the friction that might act between the backfill and the rough rock face. To increase the stiffness of the 5 mm-thick steel plate, 5 longitudinal and 5 transverse steel L-beams were welded to the back of the plate. The 30 mm × 30 mm × 3 mm steel beams were attached to establish a grid-beam system to reinforce the thin steel plate.

To evaluate the interface friction angle δ_i between the backfill and the interface plate, special direct shear tests were conducted. In the test, the lower shear box was replaced with a steel plate fully covered with a layer of anti-slip material. Air-dry Ottawa sand was pluviated into the upper shear box. To establish the relationship between the unit weight of the backfill γ and the δ_i angle, soil specimens with different unit weights were tested. Based on test results, the following empirical relationship was obtained: $\delta_i = 2.7\gamma - 21.39$, where the unit of δ_i was degree and the unit of γ was kN/m^3. The relationship was valid for γ = 15.1-16.4 kN/m^3 only. For example, if the unit weight of soil was 15.6 kN/m^3, the corresponding interface friction angle would be 20.7°. Based on his test results, Potyondy (1961) concluded that the friction force between sand structural materials was mainly affected by the roughness of the material surface and the normal force applied. In this study, the anti-slip material attached to the steel interface plate was used to simulate a flat sandstone surface. Using a direct shear test device, Canakei *et al.* (2016) studied the interface characteristics of organic soil and various solid construction materials. Test results showed that the frictional resistance between construction material and the soil is affected by the type of material and its surface roughness. Other than the direct shear test, Fang *et al.* (2004) developed a sliding block testing devise for measuring the friction at the interface between soil and different materials at low stress conditions.

To keep the interface plate stable during testing, a supporting system for the interface plate was developed. In Fig. 2, a top supporting beam was placed at the back of the interface plate. The beam was fixed at the bolt slots on the side wall of the soil bin. In Fig. 2, the bottom end of the interface plate was inserted into the

trapezoidal groove on the base support block at the horizontal distance of b = 100 mm from the base of the model wall. Six pieces of 1,860 mm-long base boards were stacked between the base support block and the end wall to keep the base block in place during testing.

3. BACKFILL AND INTERFACE CHARACTERISTICS

Air-dry Ottawa sand was used throughout this investigation. The particle distribution curve for the Ottawa sand used for all experiments in this paper is illustrated in Fig. 5. Physical properties of the soil include G_s = 2.65, e_{max} = 0.76, and e_{min} = 0.50.

For this study, the backfill was deposited by air pluviation from the slit of a hopper into the soil bin. The drop distance was approximately 1.0 m to the soil surface throughout the placement process. The soil unit weight γ achieved with the pluviation method was 15.6 kN/m^3, and its relative density D_r was 35%. The corresponding internal friction angle ϕ determined from direct shear tests was found to be 31.3°. To limit the scope of this study, only one density was used throughout all experiments.

Note that the backfill with the relative density of 35% is a very loose material. In practice, the granular backfill behind a retaining wall is generally recommended to be compacted to achieve a relative density of 70% to 75% (US Navy 1986). It should be mentioned that the test results obtained in this study are limited for the retaining wall backfilled with a loose cohesionless material.

To investigate the possible variation of density in the pluviated soil mass, several density-control cups were used. The cylindrical cup was made of acrylic with an inner diameter of 100 mm and height of 50 mm. For the density distribution experiment, the cups were placed in the soil mass at different locations and depths. Experimental results indicated that the mean relative density D_r was 35% with a standard deviation of 1.0%. From a practical point of view, it may be concluded from these test data that the soil density in the soil bin was quite uniform.

To model plane strain conditions in the laboratory, the frictional resistance between the soil and side walls of the soil box should be reduced as much as possible. Methods commonly employed for this purpose include a latex sheet with silicon grease ("grease method") or multiple layers of thin plastic sheeting ("plastic sheet method"). Fang *et al.* (2004) developed a new sliding block testing device for measuring the friction at the interface between soil and different materials at low stress conditions. Interface friction angles for eight different methods for reducing boundary friction were investigated using the proposed testing method. With the lubrication layer, the side wall friction angle could be reduced to approximately 7.5°. Test results indicated that the friction angle obtained with the plastic sheet method was nearly independent of the normal stress. On the other hand, the interface friction angle of the grease method was quite high under low normal stress conditions. Thus, the plastic sheet method appears to be a more appropriate technique under low normal stress conditions to reduce the boundary friction for laboratory scale model tests. As compared with the grease method, advantages of the plastic sheet method included constant friction angles, less time for preparation and clean-up, and lower cost.

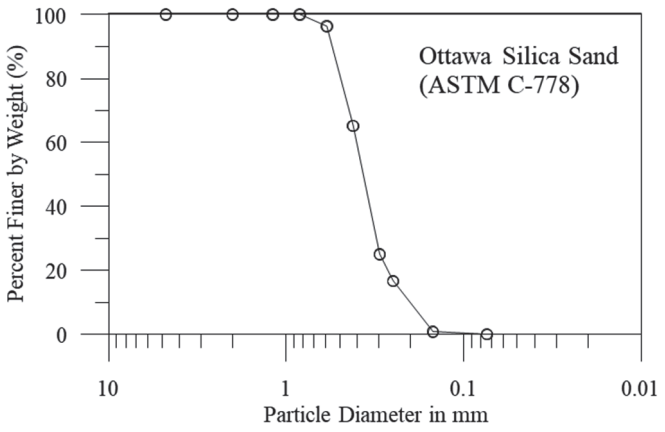

Fig. 5 Grain size distribution of Ottawa sand

4. TEST RESULTS

This section reports the experimental results regarding the effects of an adjacent inclined rock face on the active earth pressure against a retaining wall with loose cohesionless backfill. Considering the intrusion of the inclined rock face into the active soil wedge illustrated in Fig. 1, the rock face inclination angles β = 0°, 50°, 60°, 70°, 80°, 90° and the horizontal spacing b = 0, 50 mm, 100 mm were tested. For all experiments, the surface of backfill was horizontal and the height of the backfill above the wall base H was 0.5 m.

4.1 Horizontal Earth Pressure without Backfill Constraint

The variation of lateral earth pressure as a function of active wall movement was investigated. A picture of the model retaining wall facility with a horizontal backfill was shown in Fig. 6. After the loose backfill had been placed into the soil bin, the model wall slowly moved away from the soil mass in a translation mode at a constant speed of 0.015 mm/s.

Distributions of horizontal earth pressure σ_h measured at different stages of horizontal wall displacements S/H were illustrated in Fig. 7. The horizontal wall displacement S was normalized by

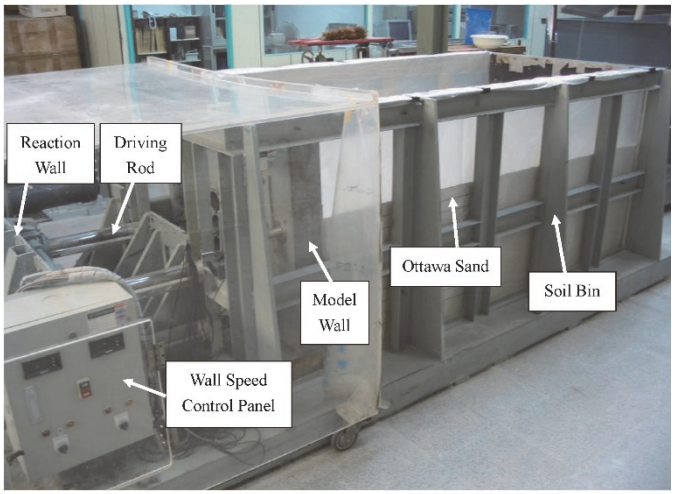

Fig. 6 Model retaining wall facility with horizontal backfill

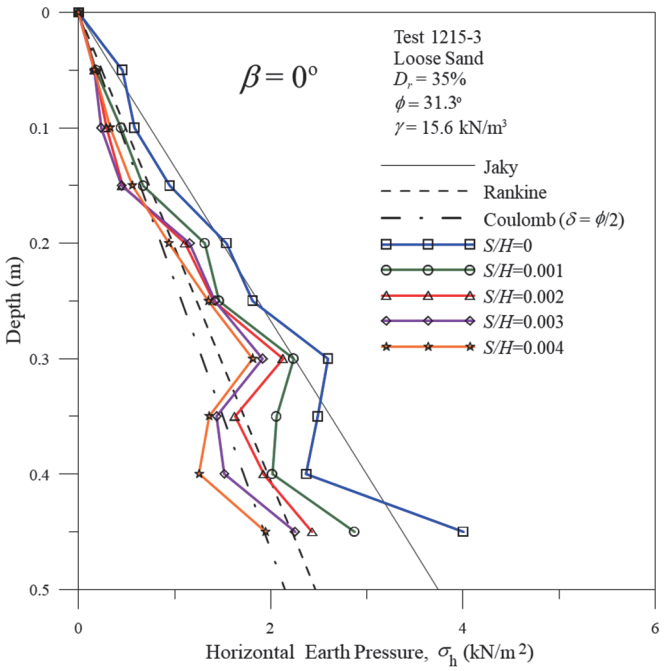

Fig. 7 Distribution of horizontal earth pressure for β = 0°

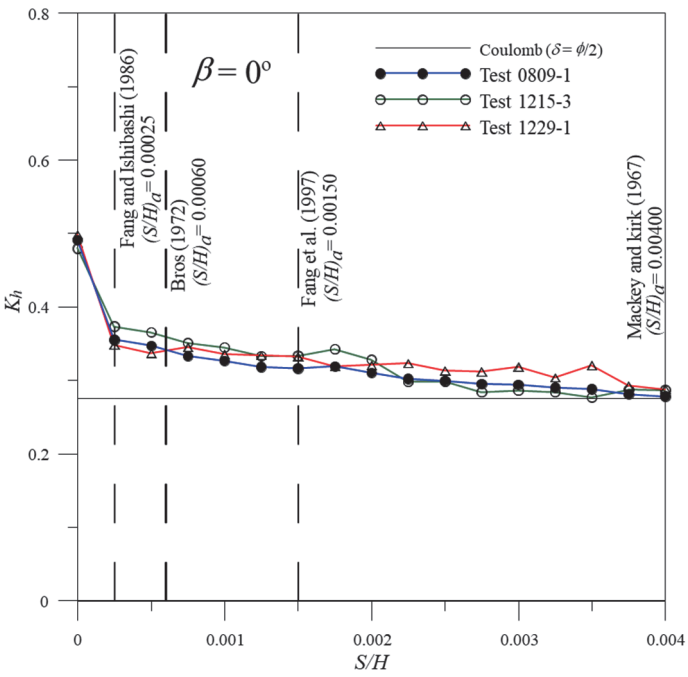

Fig. 8 Earth pressure coefficient K_h versus wall movement for β = 0°

the backfill height H. Conventionally, the earth pressure at-rest is evaluated by the Jaky equation (Jaky 1944). Based on their laboratory tests, Sherif *et al.* (1984) found that the Jaky's equation (K_o = 1 – sinϕ) gives good results when the backfill is loose sand, where K_o is the coefficient of earth pressure at-rest and ϕ is the internal friction angle of soil. As the wall started to move, the earth pressure decreased, and eventually a limit limiting active pressure was reached. Active earth pressures calculated with Rankine and Coulomb theories were also indicated in the figure. The ultimate active pressure distribution at S/H = 0.004 was relatively close to that estimated with Coulomb and Rankine theories. The fluctuation of horizontal stresses measured at the depths between z = 0.3 m and 0.4 m was most probably due to the deviation of local soil density.

The variation of horizontal earth-pressure coefficient K_h as a function of wall displacement was shown in Fig. 8. The coefficient K_h was defined as the ratio of the horizontal component of total soil force P_h to $\gamma H^2/2$. The horizontal soil resultant P_h was calculated by summing the pressure diagram shown in Fig. 7. The coefficient K_h decreased with increasing wall movement S/H until a minimum value was reached, and then remained approximately a constant. The ultimate value of K_h was defined as the horizontal active earth-pressure coefficient $K_{a,h}$. In Fig. 8, the active condition was reached at approximately S/H = 0.00375-0.004.

In Fig. 8, it may not be an easy task to define the point of active wall movement S_a. For a wall that moved away from a loose sandy backfill in a translational mode, Mackey and Kirk (1967) concluded that the wall displacement required to reach an active state was S_a = 0.004 H. The S_a values recommended by Mackey and Kirk (1967), Bros (1972), Fang and Ishibashi (1986) and Fang *et al.* (1997) were also illustrated in Fig. 8. In this study the active wall movement was assumed to be S_a = 0.004 H. It should be mentioned that only the horizontal component of the Coulomb active force was indicated in Fig. 8.

Potyondy (1961) investigated the skin friction between various soils and construction materials. It was concluded that, among several other factors, the interface friction was influenced by the roughness of the wall material. Sowers (1979) suggested that for smooth concrete the wall friction angle is often ϕ/2 to 2ϕ/3. Das (2004) stated that, in the actual design of retaining walls, the value of the wall friction angle δ was assumed to be between ϕ/2 and 2ϕ/3. For this study, the model wall was made of smooth steel, as a result the wall friction angle was assumed to be δ = ϕ/2 = 15.65°. It is obvious that, except the influence the roughness of the wall material, the wall friction angle is influenced by the soil strength. With increasing active wall movement, the loose cohesionless backfill was sheared and would contract. The density and internal friction angle of the soil would change with increasing shear strain. The variation of wall friction angle with the wall movement is beyond the scope of this study. It should be noted that the wall friction angle mentioned above was assumed only for the calculation of earth pressure for the Coulomb and Rankine theories in this paper. It may be observed in Fig. 8 that the Coulomb theory provided a fairly good estimation of the active soil thrust.

4.2 Horizontal Earth Pressure for b = 0 mm

Figures 9(a) to 9(d) showed the distributions of earth pressure at different stages of wall movement with the presence of a stiff interface plate at an inclination angle β = 50°, 60°, 70°, and 80°. Based on Jaky's equation, for ϕ = 31.3° the coefficient of earth pressure at-rest should be K_o = 0.48. In Fig. 9(a), the measured earth pressure at-rest (at S/H = 0) was lower than Jaky's solution at the lower half of the wall. At the wall movement S/H = 0.004, the active earth pressure was less than Coulomb's solution at the lower part of the wall. The test finding could be explained with the help of Fig. 4. In the picture, for the upper part of the model wall, the interface plate was relatively far from the soil pressure

transducers. It was reasonable to expect the measured active earth pressure would be close to Coulomb's prediction. However, for the lower part of the model wall, soil arching may develop in the narrow backfill between the wall and the interface. In this narrow backfill, as reported by Take and Valsangkar (2001), arching effect is the most probable reason why the measured active earth pressure was significantly lower than Coulomb's prediction.

In Fig. 9(d) for β = 80°, the interface plate was placed quite close to the model wall surface. The amount of backfill material sandwiched between the rock face and the wall was very little. At the active wall movement of 0.004 *H*, the active earth pressure measured at the lower half of the wall was obviously lower than Coulomb's solution. In Fig. 9(d), the horizontal earth pressure only slightly decreased with the active wall movement.

Figure 10 presents the variation of horizontal earth pressure coefficient K_h as a function of wall movement for various β angles. At the wall movement $S = 0$, the measured at-rest soil thrust coefficient for β = 0 was in fairly good agreement with Jaky's prediction K_o = 0.48. However, with the intrusion of the inclined face, for β = 50°, 60°, 70°, and 80°, the measured at-rest earth pressure coefficient was only 0.30, 0.27, 0.22, and 0.18, respectively. The active conditions were observed at the wall movement of approximately 0.004 *H*. In Fig. 10, the magnitude of active soil thrust which might cause a sliding failure of the wall decreased with increasing interface inclination angle β.

In the Coulomb active earth pressure theory, the forces acting on the active soil wedge included: (1) the weight of the wedge *W*; (2) the resultant *R* which inclined at an angle ϕ to the normal of the failure plane; and (3) the active force P_a. For $b = 0$, as the rock face inclination angle β increased from 50° to 80°, the soil wedge behind the wall was cut to a very small slice, the weight of the soil wedge *W* decreased significantly. As a result, the force polygon constituted of forces *W*, *R*, and P_a became much smaller, therefore the magnitude of the active force P_a decreased.

Figure 11 showed the variations of the point of application of the soil thrust as a function of wall movement for various β angles. Note that *h* is defined as the vertical distance between the point of application of total resultant and the wall base. The distance *h* is calculated by dividing the sum of moment of all measured pressure areas about the wall base by the horizontal soil resultant P_h. In Fig. 11, the location of the pressure resultant was normalized by the backfill height *H*. In Fig. 7, for β = 0 the distributions of earth

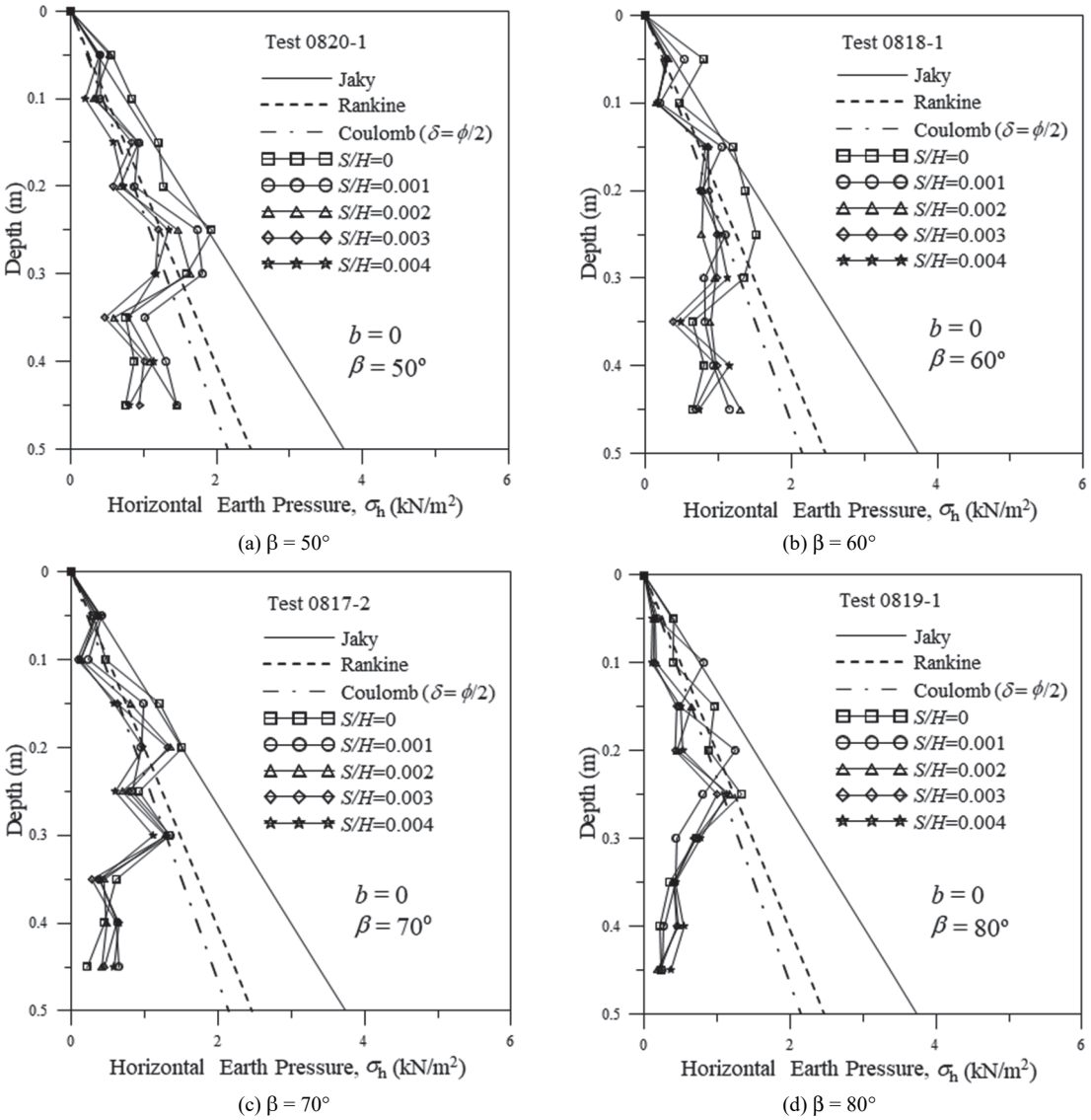

(a) β = 50° (b) β = 60°

(c) β = 70° (d) β = 80°

Fig. 9 Distribution of horizontal earth pressure for *b* = 0 and various β values

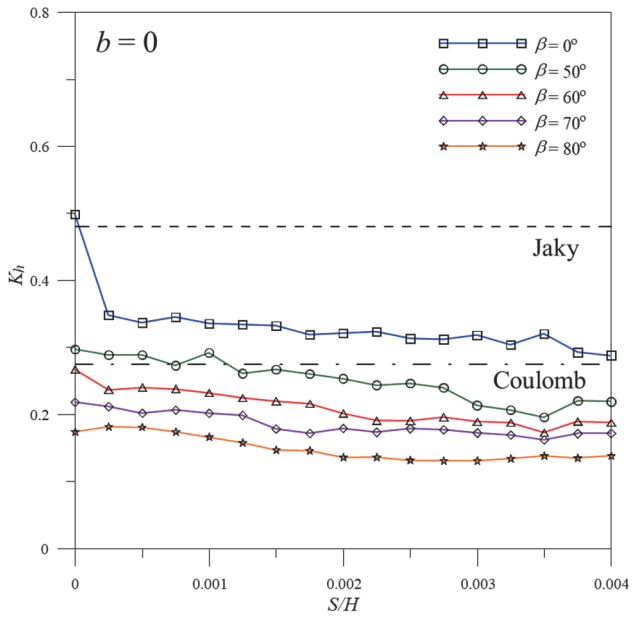

Fig. 10 Variation of K_h with wall movement for b = 0 mm

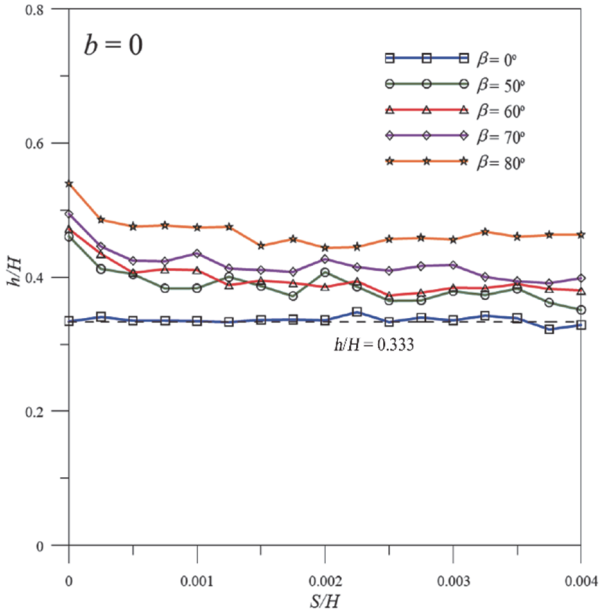

Fig. 11 Variation of h/H with wall movement for b = 0 mm

pressure at different wall movements were roughly linear. As a result, the location of the active soil thrust should act at about 0.333H above the wall base. In Fig. 11, for β = 0 (square data point and blue curve) the points of application of the soil resultant were located at about 0.33 H to 0.36 H above the wall base. At the active wall movement of 0.004 H, for β = 50°, 60°, 70°, and 80°, the active soil resultant location $(h/H)_a$ values reached 0.35, 0.38, 0.40, and 0.46, respectively. Figure 11 showed, the points of application of the active soil thrusts ascended with increasing β angle.

With the increase of β angle, the interface moved closer to the wall, and the arching effect in the soil wedge would become more significant. The reduction of vertical and horizontal stresses at the lower part of the narrow backfill due to soil arching could be the main reason why the points of application of active thrusts ascended with increasing β angle.

4.3 Horizontal Earth Pressure for b = 50 mm

Figures 12(a) to 12(e) showed the distributions of earth pressure at different stages of wall movement with the presence of a stiff rock face inclined at the angle of 50°, 60°, 70°, 80°, and 90° with the horizontal. For these tests, the horizontal spacing between the base of the interface plate and the base of the wall was b = 50 mm. Figure 13(a) showed the side-view of the model wall and the interface plate for b = 50 mm and β = 50° before backfilling, and Fig. 13(b) indicated a top-view of the soil bin after the backfill was placed. Similar pictures for b = 50 mm and β = 80° were demonstrated in Figs. 14(a) and 14(b). In Fig. 12(d), the active earth pressure on the lower part of the wall was lower than Coulomb's prediction. This phenomenon could be explained with the help of Figs. 14(a) and 14(b). Figure 14(a) showed, for b = 50 mm and β = 80°, the model wall was quite close to the inclined plate. Figure 14(b) indicated the amount of soil filled between the wall and the inclined rock face was thin. When the wall moved away, the narrow backfill gradually lost its lateral support. Based on their centrifuge test results, Take and Valsangkar (2001) reported arching was observed within the narrow backfill to truncate lateral earth pressure. Due to the arching effect, cohesionless particles formed an arch in the narrow backfill. The soil arch probably blocked the downward movement of the backfill, and the transfer of overburden normal stress in the narrow backfill. Therefore, the vertical and horizontal normal stresses in the lower part of backfill were less than Coulomb's prediction. Based on their numerical studies, Chen *et al.* (2019a) and Chen *et al.* (2019b) also reported, for rigid walls near inclined rock faces, the earth pressure on the lower part of the wall was less than Coulomb's prediction.

At the active wall movement of 0.004 H, the measured horizontal active earth pressure $\sigma_{a,h}$ was in fairly good agreement with the Coulomb's solution at the "upper part" of the wall. In Figs. 9(a) to 9(d) for b = 0, the upper part represents the upper 0.40 H to 0.55 H part. In Figs. 12(a) to 12(d) for b = 50 mm, the active pressure zone represents the upper 0.60 H to 0.80 H part. As the spacing b increases from 0 to 50 mm, the inclined rock-face slightly moves away from the wall, and the upper part grows larger. When the inclined rock-face is far away from the wall, as indicated in Fig. 6, the active pressure zone should equal to the height of backfill H.

For the interface inclination angle β = 90°, the rock face was actually parallel to the vertical model wall. Only a 0.05 m-thick backfill was sandwiched between the rock face and the retaining wall. It was impossible for the active soil wedge to develop behind the wall. As a result, both the magnitude and distribution of active earth pressure were significantly affected by the nearby rock face. For this special condition, Fig. 12(e) clearly indicated that Coulomb's solution significantly overestimated the active earth pressure on the retaining wall.

Figure 15 presented the variation of horizontal earth pressure coefficient K_h as a function of wall movement for various β angles. Test data indicated that the amount of active wall movement required to reach an active state was influenced by the degree of rock face intrusion. In this study, for comparison purposes, the active wall movement was assumed to be 0.004 H. It was clear in Fig. 15 that the active earth pressure coefficient $K_{a,h}$ decreased with increasing β angle. Figure 16 showed the variations of the location of earth pressure resultant as a function of wall movement for

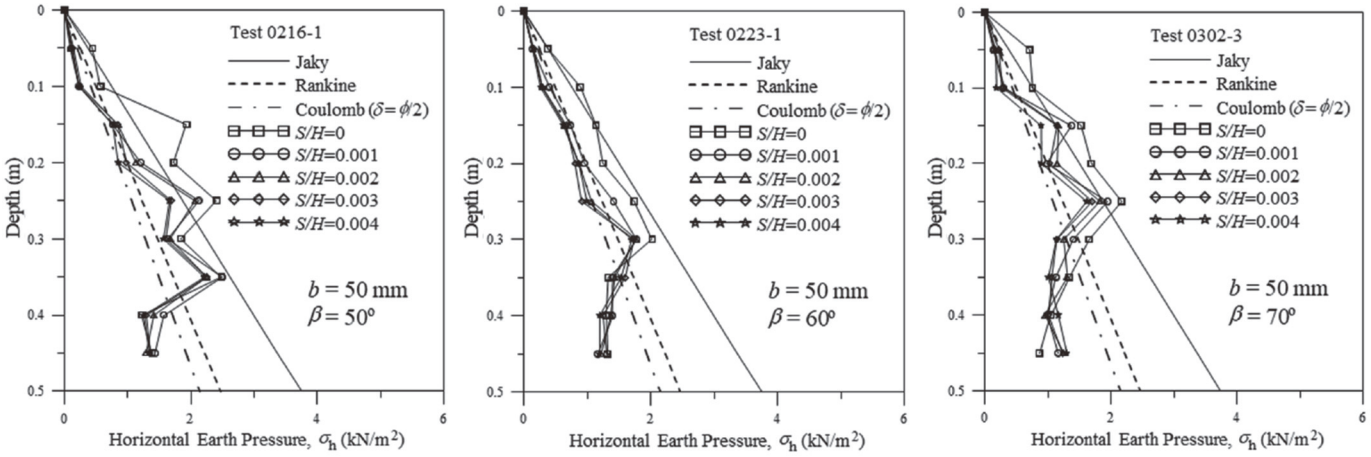

(a) β = 50° (b) β = 60° (c) β = 70°

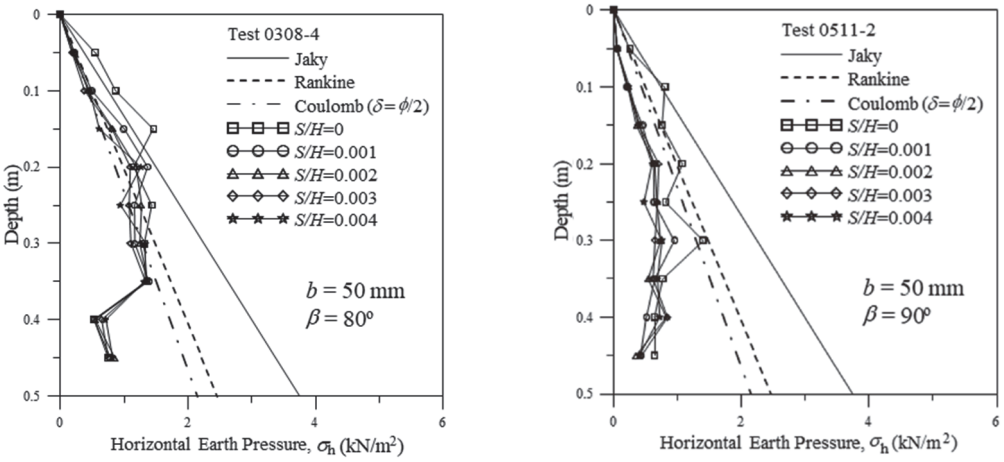

(d) β = 80° (e) β = 90°

Fig. 12 Distribution of horizontal earth pressure for b = 50 mm and various β values

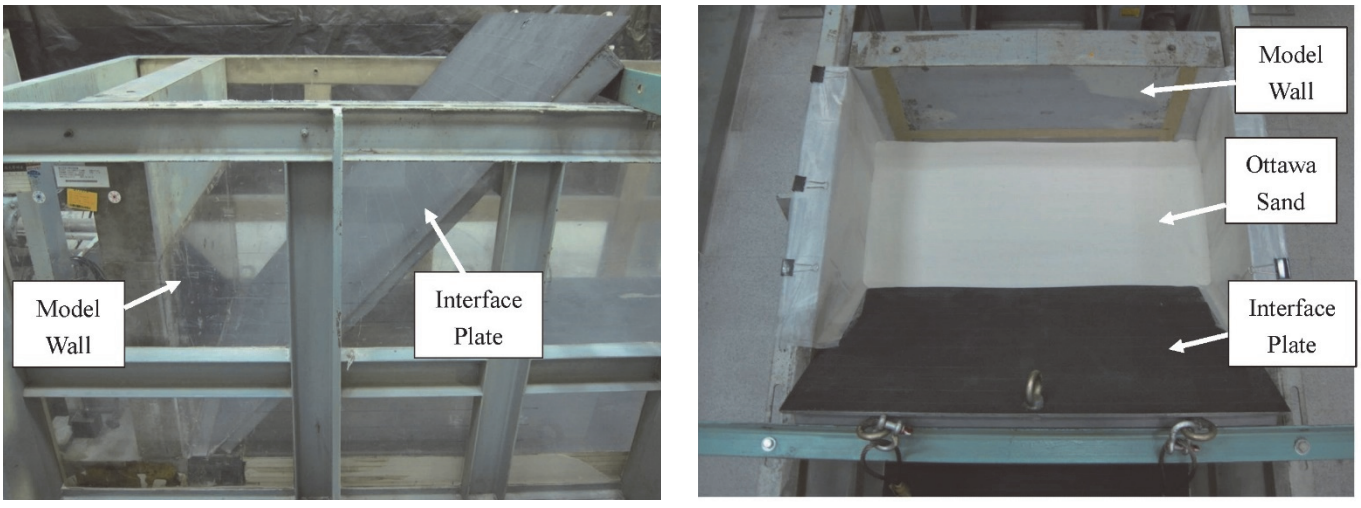

(a) (b)

Fig. 13 Model wall test: (a) side-view of model wall and interface plate for b = 50 mm and β = 50° before soil fill; (b) top-view of soil bin after backfill was placed

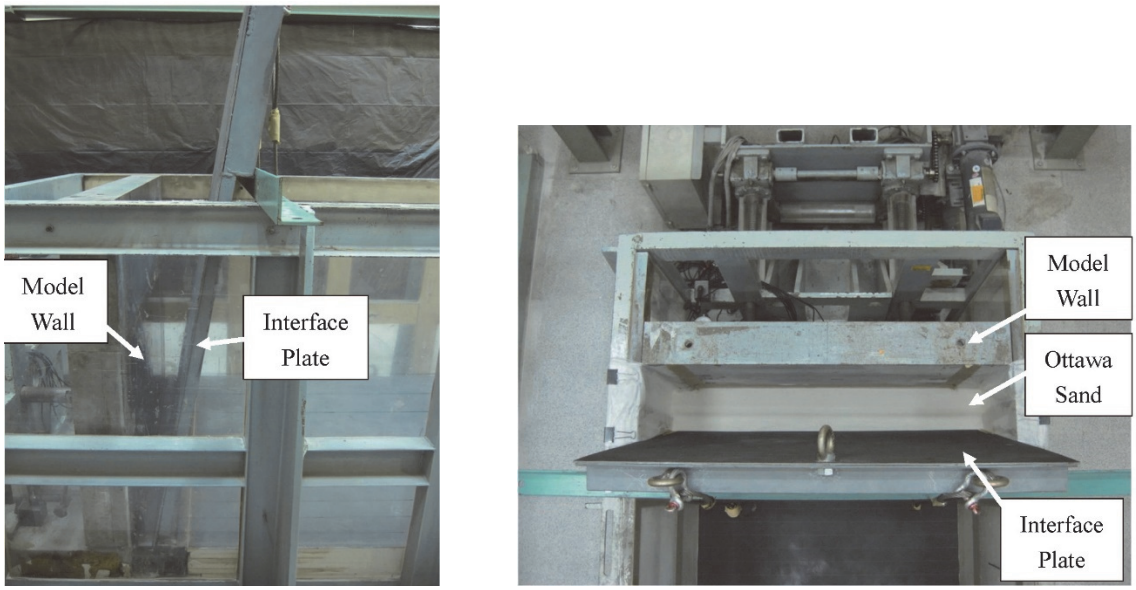

(a) (b)

Fig. 14 Model wall test: (a) side-view of model wall and interface plate for b = 50 mm and β = 80° before soil fill; (b) top-view of soil bin after backfill was placed

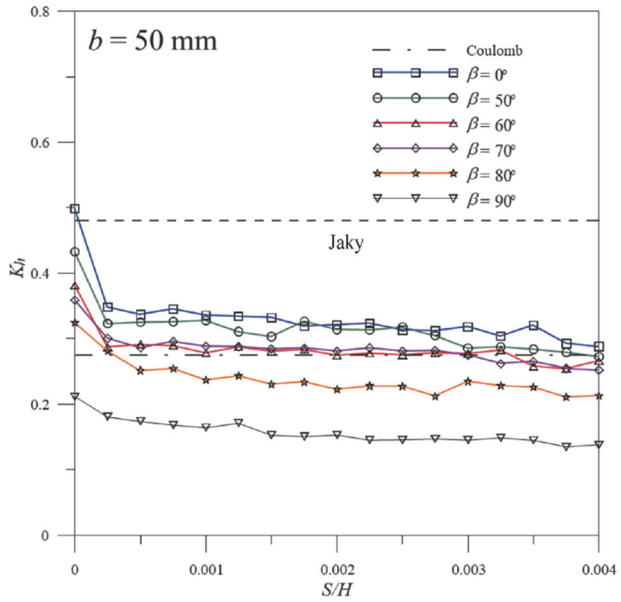

Fig. 15 Variation of K_h with wall movement for b = 50 mm

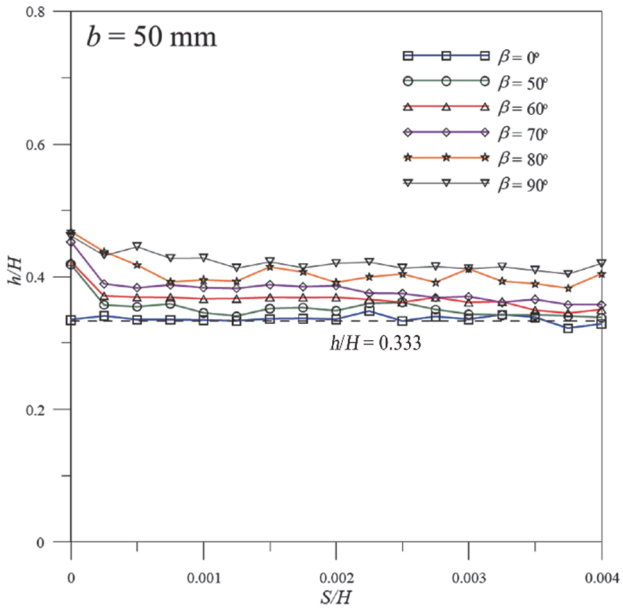

Fig. 16 Variation of h/H with wall movement for b = 50 mm

various β angles. At the active wall movement of 0.004 H, for β = 50° the active h/H value was 0.34. In the same figure, for β = 90° the location of the active soil resultant rose to 0.42 H above the wall base. It should be mentioned that the point of application of the soil thrust simply reflected the distribution of horizontal earth pressure illustrated in Fig. 12.

4.4 Horizontal Earth Pressure for b = 100 mm

Figures 17(a) to 17(e) showed the distributions of earth pressure at different stages of wall movement with the presence of an interface plate with an inclination angle from 50° to 90°. For these tests, the horizontal distance between the base of the interface plate and the base of the wall was 100 mm. In Fig. 17(a), for β = 50°, the measured active earth pressure was converging to Coulomb's solution. It was clear in Fig. 2 that with β = 50° and b = 100 mm, the interface plate was relatively far from the wall and did not intrude the active soil wedge behind the wall. As a result, the measured active earth pressure was not significantly affected by the presence of the inclined rock face.

For β = 90°, the rock face was parallel to the vertical wall. It was impossible for the active soil wedge to develop in the 0.1 m-thick backfill which was sandwiched between the interface plate and the retaining wall. In Fig. 17(e), the distribution of active earth pressure against the lower half of the wall was significantly lower than Coulomb's solution. It should be mentioned that, it is not

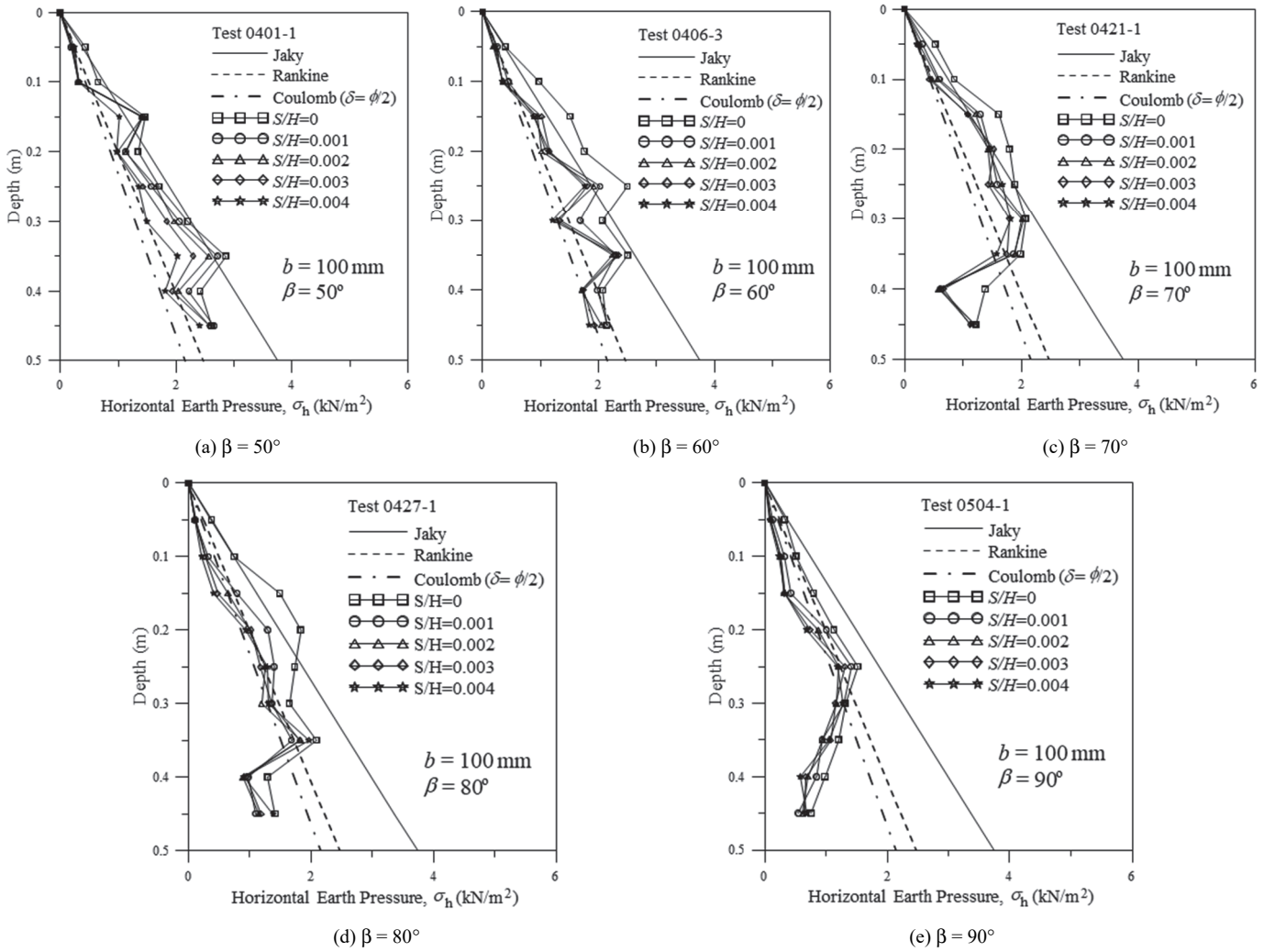

(a) β = 50° (b) β = 60° (c) β = 70°

(d) β = 80° (e) β = 90°

Fig. 17 Distribution of horizontal earth pressure for *b* = 100 mm and various β values

appropriate to use the Coulomb theory to estimate the lateral earth pressure acting on narrow parallel boundaries. The Coulomb solutions shown in Figs. 12(e) and 17(e) were used for comparison purposes only.

Figure 18 showed the variation of earth pressure coefficient K_h with wall movement for various β angles. For b = 100 mm and β = 50° (circular data points and green curve), the interface plate was relatively far from the soil pressure transducers. As indicated in Fig. 2, the active soil wedge was not significantly affected by the inclined rock face. Therefore, for β = 50°, 60°, and 70°, the magnitudes of the active soil thrust were quite close to the value predicted by Coulomb. However, for β = 90°, the vertical interface plate was only 0.1 m horizontally from the model wall, therefore the measured $K_{a,h}$ was significantly lower than the value estimated with Coulomb's theory. The variations of h/H as a function of wall movements for various β angles were shown in Fig. 19. For β = 50° and 90°, the active soil thrust was located at about 0.34 H and 0.38 H above the wall base, respectively.

4.5 Comparison of Research Findings

To design a storage silo filled with granular material, it is important for the designer to know how much lateral pressure is acting on the inside of the silo wall. The granular material in the silo is generally constrained by the parallel vertical walls. At an active condition, the movable model wall simulates the vertical silo wall which yields laterally under the internal pressure. At β = 90°, the steel interface plate simulates the vertical central axis of the silo that remains unyielding due to symmetry.

In Fig. 20, the horizontal earth pressure was normalized with the vertical stress σ_v. In the model retaining test by Chen and Fang (2008), dry Ottawa sand was placed with air-pluviation method. It was reported that vertical pressure in the soil mass increased linearly with increasing depth z. The test data were in good agreement with the predicted distribution using the tradition equation $\sigma_v = \gamma z$, where γ = unit weight of backfill.

Figure 20 showed the distribution of normalized horizontal active pressure ($\sigma_{a,h}/\gamma z$) based on the theoretical solution by Spangler and Handy (1984) and the numerical solution reported by Fan and Fang (2010), where z is the depth measured from the soil surface. The element size in the backfill behind the retaining wall was about 0.15 to 0.17 m in the finite element modeling. For an 8.5 m-high wall adjacent to a vertical rock face with b = 1.0 m in the numerical analysis, deformations of the soil element at the top and bottom of the backfill after the backfilling and prescribed horizontal wall movement (0.005 H) to reach the active state, were about

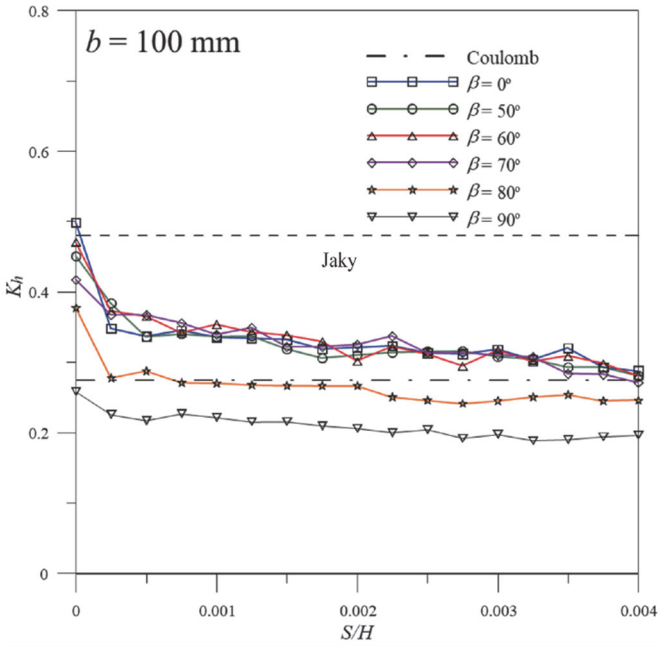

Fig. 18 Variation of K_h with wall movement for b = 100 mm

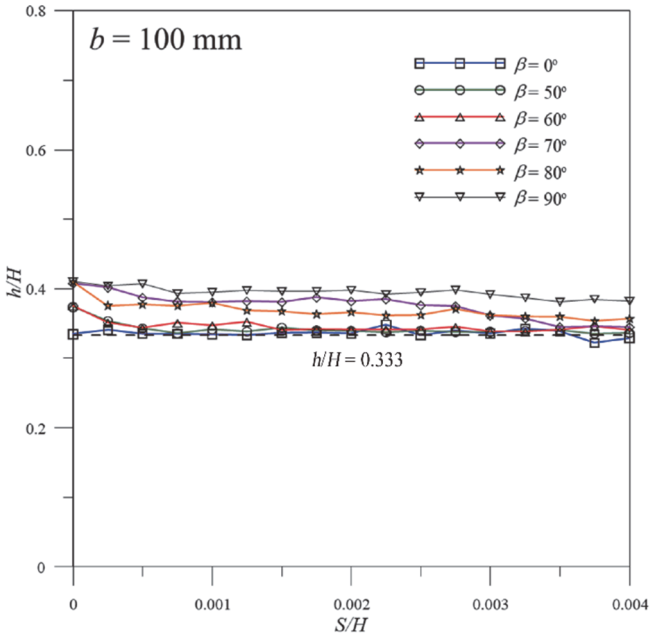

Fig. 19 Variation of h/H with wall movement for b = 100 mm

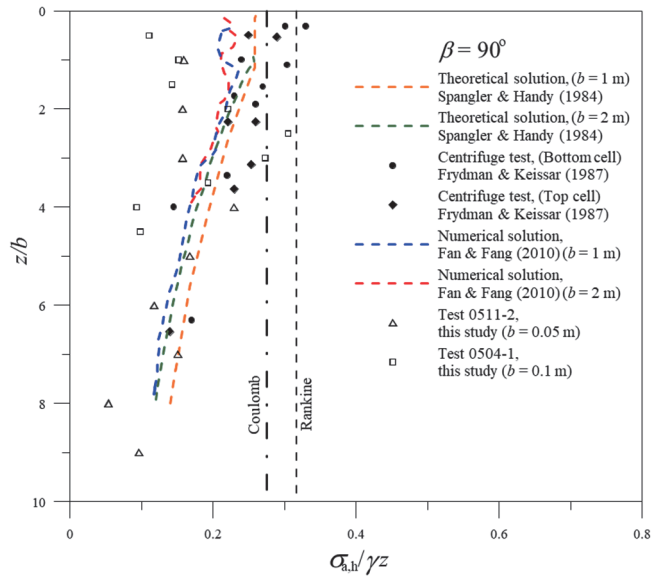

Fig. 20 Comparison of the distribution of active earth pressure for β = 90°

0.26 m and 0.035 m, respectively. Experimental results based on centrifuge tests by Frydman and Keissar (1987) and the 1-g physical model tests of this study were also included. In Fig. 20, with a constrained backfill, the normalized active pressure $\sigma_{a,h}/\gamma z$ was not a constant with increasing depth, it decreased with depth. For the most parts, the theoretical, numerical and experimental results were in relatively good agreement. It can be concluded that, with constrained backfill, both Coulomb and Rankine theories would overestimate the active earth pressure against the vertical silo wall.

It should be noted that, in the silo problem the arching effects are dominant, and the application of Coulomb and Rankine analysis would not be appropriate. In Fig. 20, the Rankine and Coulomb solutions were indicated for comparison purposes only.

5. DESIGN CONSIDERATIONS

In the design of a rigid retaining structure, it is often necessary to check its adequacy. Besides several other criteria, the NAVFAC Design Manual DM-7.02 (US Navy 1986) required the designer to check its resistance against sliding and overturning. It is important for the designer to evaluate how the nearby inclined rock face influences the factor of safety against sliding and overturning of the retaining wall.

5.1 Factor of Safety against Sliding

The factor of safety against sliding (FS_{sliding}) was defined as:

$$FS_{\text{sliding}} = \frac{\sum F_R}{\sum F_D} \tag{2}$$

where $\sum F_R$ = the sum of horizontal resisting forces and $\sum F_D$ = the sum of horizontal driving forces. For the retaining wall shown in Fig. 1, the horizontal driving force on the wall was the horizontal component of the active soil force. The horizontal active earth pressure coefficient $K_{a,h}$ as a function of β angle for b = 0, 0.1 H, and 0.2 H were shown in Fig. 21. For comparison purposes, the numerical solutions reported by Fan and Fang (2010) were also indicated in the figure. Without backfill constrain (β = 0), the experimental $K_{a,h}$ coefficient was quite close to Coulomb's solution. For b = 0.1 H and 0.2 H, the experimental $K_{a,h}$ values were in good agreement with the numerical findings. In Fig. 21, the magnitude of active force decreased with increasing β angle. Although the trend was similar, for b = 0, the experimental $K_{a,h}$ coefficients were lower than the numerical $K_{a,h}$ values. The interface friction angle δ_i between the wall and the backfill in the numerical study was 28°, while the δ_i value in the experimental work was 20.7°. In addition, to avoid the interference of the soil elements and interface elements around the bottom corner of the backfill, a width of b = 0.1 m was assigned at the bottom of the backfill in the numerical analysis. The soil arching was most significant for the constrained

backfill with b = 0. These issues might cause the difference between the numerical and experimental results for b = 0.

In Fig. 21, the horizontal active earth pressure coefficient $K_{a,h}$ decreased with increasing rock face inclination angle β. Why does the magnitude of active soil thrust decrease with the approach of the inclined rock face? This may be explained by the soil arching effect reported by Spangler and Handy (1984), Janssen (1895), Frydman and Keissar (1987), Zhang *et al.* (1998) and Take and Valsangkar (2001). It was found that in the soil mass between narrow faces, inclined or not, arching effect appeared. In Fig. 2, the confined backfill was bounded by the retaining wall and the inclined rock face. The inclined rock face provided another frictional surface for the cohesionless backfill. Due to arching effect in the confined soil mass, the vertical component of frictional boundary stress will reduce the geostatic vertical stress, which will in turn reduce the horizontal stress acting on the wall. This is part of the reasons why the active earth force acting on the wall decreased with the approach of the inclined rock face.

In Eq. (2), if the driving force on the wall was reduced and the resisting force remained the same, the factor of safety against sliding would increase. From a practical point of view, the constrained backfill would result in a greater *FS* against sliding. In other words, the evaluation of *FS* against sliding with Coulomb's theory would be on the safe side. However, if the inclined rock face was vertical and located very close to the retaining wall (for example b = 0.1 H), Coulomb's solution could overestimate the active soil force for approximately 100%. Based on Eq. (2), the theoretical *FS* against sliding would be twice the actual *FS* against sliding.

5.2 Factor of Safety against Overturning

The factor of safety against overturning was expressed by the following equation:

$$FS_{\text{overturning}} = \frac{\sum M_R}{\sum M_O} \tag{3}$$

where $\sum M_R$ = the sum of resisting moments and $\sum M_O$ = the sum of overturning moments about toe. The overturning moment in Eq. (3) is the product of the horizontal active force $P_{a,h}$ and the moment arm h. To obtain dimensionless quantities for comparison, the horizontal active resultant $P_{a,h}$ was normalized with $\gamma H^2/2$ and the moment arm h was normalized with the wall height H. The normalized moment arms h/H as a function of β angle for b = 0, 0.1 H, and 0.2 H were shown in Fig. 22. The numerical findings reported by Fan and Fang (2010) were also indicated in the figure. Both experimental and numerical results indicated that the point of application of the active soil thrust ascended with increasing β angle.

Figure 23 showed the normalized overturning moment $K_{a,h} \times (h/H)_a$ as a function of the β angle. For the data obtained with both

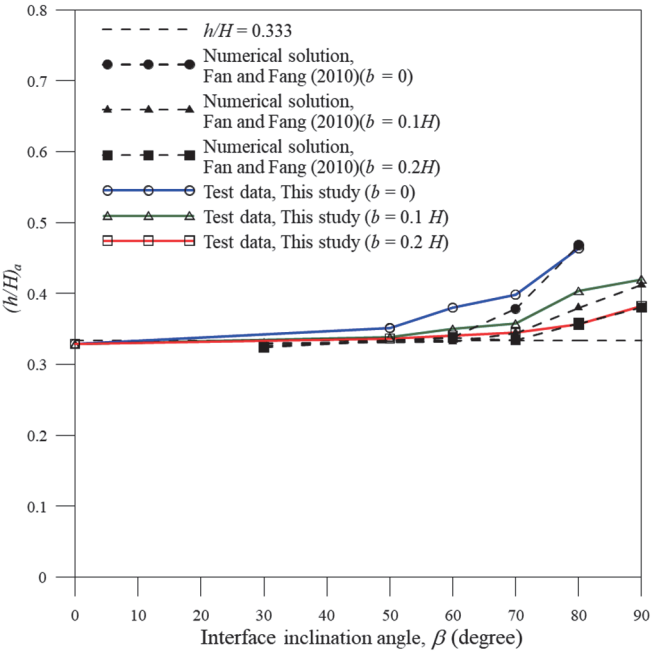

Fig. 22 Point of application of active soil thrust versus β

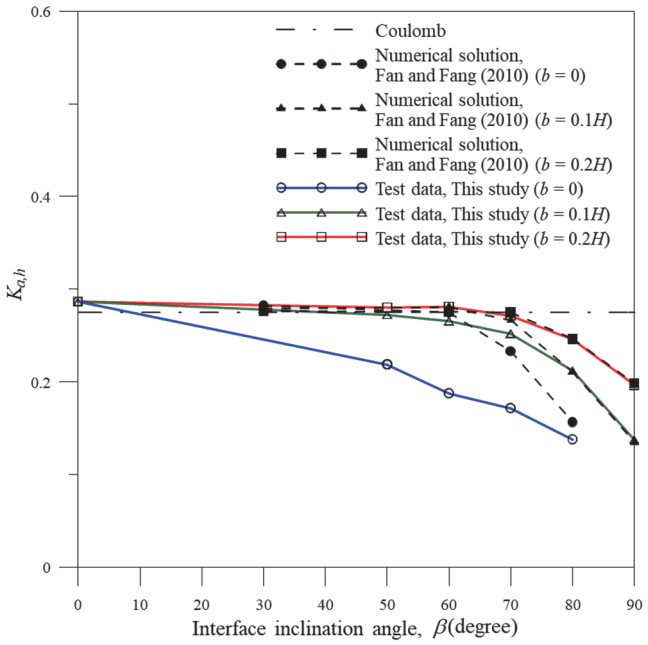

Fig. 21 Active earth pressure coefficient $K_{a,h}$ versus β

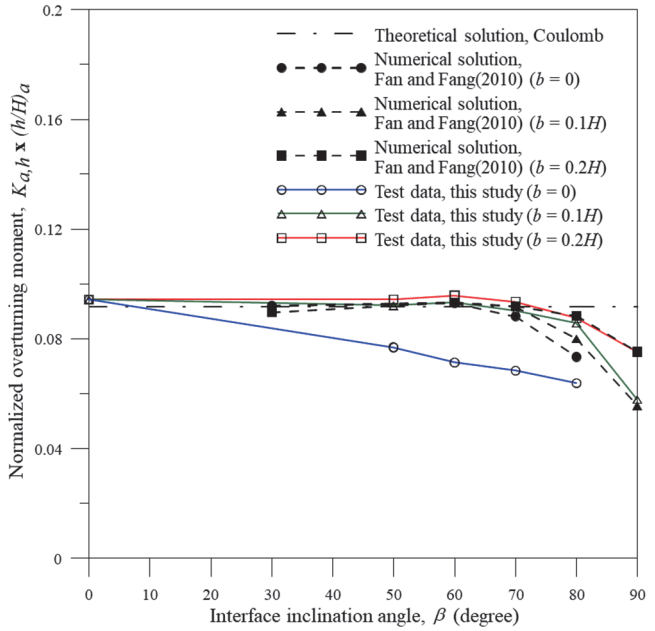

Fig. 23 Normalized overturning moment versus β

the experimental and numerical methods, the overturning moment due to the active soil thrust decreased with increasing β angle.

If the resisting moment remained the same and the overturning moment was reduced, the factor of safety against overturning calculated with Eq. (3) would increase. Test results indicated that, the existence of a nearby inclined rock face would increase the factor of safety against overturning. For the retaining wall with restricted backfill, the estimation of the factor of safety against overturning with Coulomb's theory would be on the safe side. If the interface was vertical and located very close to the wall (for example $b = 0.1\ H$ and $\beta = 90°$), Coulomb's solution could overestimate the overturning moment up to 60%.

It should be mentioned that, the calculation of the factors of safety against sliding and overturning, only the reduction of the horizontal soil thrust was considered. The influence of the vertical earth force acting on the wall was not taken into account. With the possible existence of soil arching in the backfill, the downward vertical force acting on the retaining wall might increase. This extra downward resisting drag could further increase the factors of safety against sliding and overturning of the wall.

6. CONCLUSIONS

This paper reports the experimental results regarding the effects of an adjacent inclined rock face on the active earth pressure acting on a rigid wall backfilled with loose Ottawa sand. Based on the experimental data obtained during this study, the following conclusions can be drawn.

1. Without a nearby rock face, the earth pressure decreased with increasing wall movement, and eventually a limiting active pressure was reached. For the wall with loose backfill, the ultimate pressure was measured at the active wall movement of 0.004 H. The measured active pressure distribution was relatively close to Coulomb's solution.
2. For the wall with a nearby (for example $b = 0$) inclined rock face, the active earth pressure measured at the upper part of the wall was in good agreement with Coulomb's prediction. However, the active pressure measured at the lower part of the wall was less than Coulomb's solution.
3. For $b = 50$ mm and $\beta = 90°$, the rock face was actually parallel with the vertical model wall. Only a 50 mm-thick backfill was sandwiched between the rock face and the retaining wall. It was impossible for the active soil wedge to develop behind the wall. As a result, the measured active earth pressure was significantly less than Coulomb's solution.
4. The magnitude of active force decreased with increasing interface inclination angle β. The existence of a nearby inclined rock face would result in a greater factor of safety against sliding. The evaluation of the factor of safety against sliding with Coulomb's theory would be on the safe side. However, if the inclined rock face was vertical and located very close (for example $b = 0.1\ H$) to the retaining wall, Coulomb's solution would overestimate the active soil force for approximately 100%.
5. For $b = 0$, 0.1 H, and 0.2 H, the point of application of the active soil force ascended with increasing β angle.
6. The overturning moment due to the active soil force decreased with increasing β angle. The existence of a nearby inclined rock face would increase the factor of safety against overturning of the wall. The estimation of the factor of safety against overturning with Coulomb's theory would be on the safe side. If the inclined rock face was vertical and located very close (for example $b = 0.1\ H$) to the wall, Coulomb's solution could overestimate the overturning moment up to 60%.

ACKNOWLEDGEMENTS

The authors would like to express their gratitude to Dr. Tsang-Jiang Chen, Mr. Shih-Ta Hsu and Mr. Yu-Lun Chien of the Department of Civil Engineering, National Chiao Tung University, for their kind assistance.

FUNDING

The authors wish to acknowledge the National Science Council of the Taiwan (R.O.C.) government (NSC 96-2221-E-009-004) for the financial assistance that made this investigation possible.

DATA AVAILABILITY

The data generated in this study are available from the corresponding author on reasonable request.

CONFLICT OF INTEREST STATEMENT

The authors declare that there is no conflict of interest.

NOTATIONS

b	horizontal distance between interface plate base and wall (mm)
B	backfill width (mm)
D_r	relative density (%)
e_{max}	maximum void ratio
e_{min}	minimum void ratio
F_D	driving force (kN)
F_R	resisting force (kN)
$FS_{sliding}$	factor of safety against sliding
$FS_{overturning}$	factor of safety against overturning
g	gravitational acceleration (m/s^2)
G_s	specific gravity
h	height of soil thrust above wall base (mm)
$(h/H)_a$	normalized height of active soil thrust
H	height of backfill (mm)
K	coefficient of lateral earth pressure
K_o	coefficient of earth pressure at-rest
K_a	coefficient of active earth pressure
$K_{a,h}$	coefficient of horizontal active earth pressure
K_h	coefficient of horizontal earth pressure
M_D	driving moment (kN-m)
M_R	resisting moment (kN-m)
P_a	active force (kN)
$P_{a,h}$	horizontal active force (kN)
P_h	horizontal soil force (kN)

S	horizontal wall displacement (mm)
S_a	horizontal active wall displacement (mm)
W	weight (kN)
z	depth (m)
β	rock face inclination angle (°)
δ	wall friction angle (°)
δ_i	inclined rock face friction angle (°)
ϕ	internal friction angle (°)
γ	unit weight (kN/m^3)
μ	friction coefficient between soil and wall
$\sigma_{a,h}$	horizontal active earth pressure (kN/m^2)
σ_v	vertical earth pressure (kN/m^2)
σ_h	horizontal earth pressure (kN/m^2)

REFERENCES

Bros, B. (1972). ‘‘The influence of model retaining wall displacements on active and passive earth pressure in sand.” *Proceedings of the 5th European Conference on Soil Mechanics*, Madrid, Spain, 241-249.

Canakei, H., Hamed, M., Celik, F., Sidik, W., and Eviz, F. (2016). “Friction characteristics of organic soil with construction materials.” *Soils and Foundations*, **56**(6), 965-972. http://doi.org/10.1016/j.sandf.2016.11.002

Chen, T.J. and Fang, Y.S. (2008). “Earth pressures due to vibratory compaction.” *Journal of Geotechnical and Geoenvironmental Engineering*, ASCE, **134**(4), 437-444. https://doi.org/10.1061/(ASCE)1090-0241(2008)134:4(437)

Chen, F., Lin, Y., and Li, D. (2019a). “Solution to active earth pressure of narrow cohesionless backfill against rigid retaining walls under translation mode.” *Soil and Foundations*, **59**, 151-161. https://doi.org/10.1016/j.sandf.2018.09.010

Chen, F., Yang, J., and Lin, Y. (2019b). “Active earth pressure of narrow granular backfill against rigid retaining wall near rock face under translation mode.” *International Journal of Geomechanics*, ASCE, **19**(12), 04019133. https://doi.org/10.1061/(ASCE)GM.1943-5622.0001525

Das, B.M. (2004). *Principles of Foundation Engineering*. 5th Edition, Brooks/Cole-Thomas Learning, Pacific Grove, CA, USA.

Fan, C.C. and Fang, Y.S. (2010). “Numerical solution of active earth pressures on rigid retaining walls built near rock faces.” *Computers and Geotechnics*, **37**, 1023-1029. https://doi.org/10.1016/j.compgeo.2010.08.004

Fang, Y.S. and Ishibashi, I. (1986). “Static earth pressures with various wall movements.” *Journal of Geotechnical Engineering*, ASCE, **112**(3), 317-333. https://doi.org/10.1061/(ASCE)0733-9410(1986)112:3(317)

Fang, Y.S., Chen, J.M., and Chen, C.Y. (1997). “Earth pressures with sloping backfill.” *Journal of Geotechnical and Geoenvironmental Engineering*, ASCE, **123**(3), 250-259. https://doi.org/10.1061/(ASCE)1090-0241(1997)123:3(250)

Fang, Y.S., Chen, T.J., and Wu, B.F. (1994). “Passive earth pressures with various wall movements.” *Journal of Geotechnical Engineering*, ASCE, **120**(8), 1307-1323. https://doi.org/10.1061/(ASCE)0733-9410(1994)120:8(1307)

Fang, Y.S., Ho, Y.C., and Chen, T.J. (2002). “Passive earth pressure with critical state concept.” *Journal of Geotechnical and Geoenvironmental Engineering*, ASCE, **128**(8), 651-659. https://doi.org/10.1061/(ASCE)1090-0241(2002)128:8(651)

Fang, Y.S., Chen, T.J., Holtz, R.D., and Lee, W.F. (2004). “Reduction of boundary friction in model tests.” *Geotechnical Testing Journal*, **27**(1), 1-10. https://doi.org/10.1520/GTJ10812

Frydman, S. and Keissar, I. (1987). “Earth pressure on retaining walls near rock faces.” *Journal of Geotechnical Engineering*, ASCE, **113**(6), 586-599. https://doi.org/10.1061/(ASCE)0733-9410(1987)113:6(586)

Jaky, J. (1944). “The coefficient of earth pressure at rest.” *Journal of Society of Hungarian Engineering and Architecture*, Budapest, 355-358. (in Hungarian)

Janssen, H.A. (1895). “Versuche uber getreidedruck in silozellen.” *Aeitschrift*, Verein Deutscher Ingenieure, **39**, 1045-1049. (in German, Partial English translation, *Proceedings of the Institute of Civil Engineers*, London, England, 1896, 553)

Leshchinsky, D., Hu, Y., and Han, J. (2004). “Limited reinforced space in segmental retaining walls.” *Geotextiles and Geomembranes*, **22**, 543-553. https://doi.org/10.1016/j.geotexmem.2004.04.002

Mackey, R.D. and Kirk, D.P. (1967). “At rest active and passive earth pressures.” *Proceedings of the South East Asian Conference on Soil Mechanics and Foundation Engineering*, Bangkok, Thailand, 187-199.

Potyondy, J.G. (1961). “Skin friction between various soils and construction materials.” *Geotechnique*, **11**, 329-353. https://doi.org/10.1680/geot.1961.11.4.339

Sherif, M.A., Fang, Y.S., and Sherif, R.I. (1984). “K_a and K_o behind Rotating and Non-yielding Walls.” *Journal of Geotechnical Engineering*, ASCE, **110**(1), 41-56. https://doi.org/10.1061/(ASCE)0733-9410(1984)110:1(41)

Sowers, G.F. (1979). *Introductory Soil Mechanics and Foundations: Geotechnical Engineering*. 4th Edition, MacMillan Publishing Co. Inc., New York, NY, USA.

Spangler, M.C. and Handy, R.L. (1984). *Soil Engineering*. 4th Edition, Harper and Row, New York, NY, USA.

Take, W.A. and Valsangkar, A.J. (2001). “Earth pressures on unyielding retaining walls of narrow backfill width.” *Canadian Geotechnical Journal*, **38**(6), 1220-1230. https://doi.org/10.1139/t01-063

US Navy. (1986). *Foundations and Earth Structures, NAVFAC Design Manual DM-7.02*, Naval Facilities Engineering Command, Washington DC, USA.

Xie, M., Zheng, J., Zhang, R., Cui, L., and Miao, C. (2020). “Active earth pressure on rigid retaining walls built near rock faces.” *International Journal of Geomechanics*, ASCE, **20**(6), 04020061. https://doi.org/10.1061/(ASCE)GM.1943-5622.0001675

Yang, K.H. and Liu, C.N. (2007). “Finite element analysis of earth pressures for narrow retaining walls.” *Journal of GeoEngineering*, **2**(2), 43-53. https://doi.org/10.6310/jog.2007.2(2).1

Zhang, J.M., Shamoto, Y., and Tokimatsu, K. (1998). “Evaluation of earth pressure under any lateral deformation.” *Soils and Foundations*, **38**(1), 15-33. https://doi.org/10.3208/sandf.38.15